



IJRASET

International Journal For Research in
Applied Science and Engineering Technology



INTERNATIONAL JOURNAL FOR RESEARCH

IN APPLIED SCIENCE & ENGINEERING TECHNOLOGY

Volume: 7 Issue: VI Month of publication: June 2019

DOI: <http://doi.org/10.22214/ijraset.2019.6222>

www.ijraset.com

Call:  08813907089

E-mail ID: ijraset@gmail.com

Characterization of AL AERO Alloy (AA2618) at Different Temperatures

K. Santosh Phanindra Kumar¹, Dr.J.Suresh Kumar²

¹Student, ²Professor, Department of Mechanical Engineering, JNTUH college of Engineering, Kukatpally, Hyderabad, India

Abstract: *The advancement of aircraft and rocket technology is directly tied to the advancement and production of aluminium alloys. From the Wright brothers' use of aluminium in the engine of their first biplane to NASA's use of an aluminium-lithium alloy in the new Orion spacecraft—aluminium has created the potential for mankind to fly both around the Earth and into space. Ever since the launch of Sputnik a half-century ago, aluminium has been the material of choice for space structures of all types. Chosen for its light weight and its ability to withstand the stresses that occur during launch and operation in space, aluminium has been used on Apollo spacecraft, the Skylab, the space shuttles and the International Space Station. Aluminium alloys consistently exceed other metals in such areas as mechanical stability, dampening, thermal management and reduced weight. In the development of Al alloys, proper temperatures and solution proportions are involved to vary the mechanical properties. The optimum heat treatment conditions are verified by determining various parameters of governing equations. Also the workability of Al alloys is measured by strain hardening exponent which is determined by performing functional fitting of experimental data thus confirming the validation of heat treatment process. Moreover, different proportions of other additives into wrought Al also varies the properties and their adaptability to higher temperatures. It is clear that a correlation as well as demarcation between monotonic and cyclic behaviour with respect to various flow parameters in standard heat treatment condition is vital to optimize the properties. The present work focusses on two different heat treated Al alloys and comparison of their parameters at different temperatures by fitting the available tensile and fatigue data to governing equations.*

I. INTRODUCTION

Aero Engines are the type of external combustion heat engines which take the ambient air, compresses it to high temperatures, and later on combusted with fuel and provides the required thrust or power to move. So in this regard there are different temperatures are involved and it is not possible to use only one type of alloys or materials in all the sections, as the temperature exceeds very much and it may reach almost near to melting point. In considering different materials for different components, weight becomes prime factor to control and it must be optimised. So in this regard we need compromise with the following:

- A. Mechanical properties
- B. Weight as well as life of component.
- C. Retaining the properties at higher temperatures.
- D. Corrosion and oxidation resistance
- E. Creep resistance

Hence to compromise above points we will go for Non Ferrous alloys, Al is major among them. Al is a versatile metal with unique characteristics and has very much substituted other metals such as copper, steel and iron in lot of applications. By adding alloying elements to Al and by undergoing heat treatment, material properties and characteristics such as yield strength, workability can be significantly altered. Commercially pure aluminium has a tensile strength of about 13,000 psi, but its strength may be approximately doubled by rolling or other cold working processes. By alloying with other metals, or by using heat-treating processes, the tensile strength may be raised to as high as 65,000 psi or to within the strength range of structural steel. Aluminium casting alloys are divided into two basic groups. In one, the physical properties of the alloys are determined by the alloying elements and cannot be changed after the metal is cast. In the other, the alloying elements make it possible to heat treat the casting to produce the desired physical properties. The primary goal of this paper is finding the effect of strain rates and temperature on tensile properties, and fracture behaviour of solution treated and solution treated+ artificially aged AA2618. Understanding of high cycle fatigue (HCF) behaviour in order to mitigate the negative impact of HCF on aerospace operations. This information is drawn out by analysing the data obtained after testing of several specimens. Wilson and Forsyth [1] investigated the effects of adding 1 wt.% nickel to an age-hardening Al-2.5%Cu-1.2%Mg alloy and found that the nickel formed an intermetallic phase which

was present from the casting stage and was insoluble at the solution-treatment temperature. After forging and rolling, the as-cast structure was broken down and the insoluble phase dispersed in the form of small spherical particles (0.5-1 μm dia.) throughout the matrix. A comparison of the final grain size achieved in the alloys after solution-treatment showed that the nickel-bearing alloys had resisted grain growth, and thin-foil transmission electron microscopy revealed that many grain boundaries were pinned by the nickel-rich particles. Feng et al [2] and Wang et al [3] investigated the microstructure of the as-cast Al-2.24Cu-1.42Mg-0.9Fe-0.9Ni alloy and found that the microstructures of the as-cast alloy consist of α -Al matrix as well as Al_2CuMg , Al_2Cu , Al_9FeNi , $\text{Al}_7\text{Cu}_2\text{Fe}$ and $\text{Al}_7\text{Cu}_4\text{Ni}$ intermetallic phases. Oguocha et al [4] reported the Al_xFeNi phase in cast AA2618 alloy has a C-centred monoclinic structure and the structural formula of this phase varies from particle to particle according to the aluminium content. A tensile test curve contains two parts—one elastic part and one plastic part. From a simulation and modelling point of view, it is desirable to be able to approximate the flow stress values with equations. Instead of performing the actual tensile test to retrieve the data. The elastic part of a tensile test curve can be approximated easily using Hooke's law, whereas the plastic part is a bit harder to approximate. Some constituent relationships are used to approximate the plastic deformation, for example, Hollomon, [5] Ludwik, [6] Ludwikson, [7]. The problem with the approximation of the plastic part is to get a valid approximation for all regions of the curve (i.e., for small plastic strains as well as for near fracture strains). These constituent relationships are general and valid for most types of materials; however, some are suited better for certain materials. Reasons for the difference in validity might be as follows: the material is brittle, there is no strain hardening, or the material forms a necking before fracture.

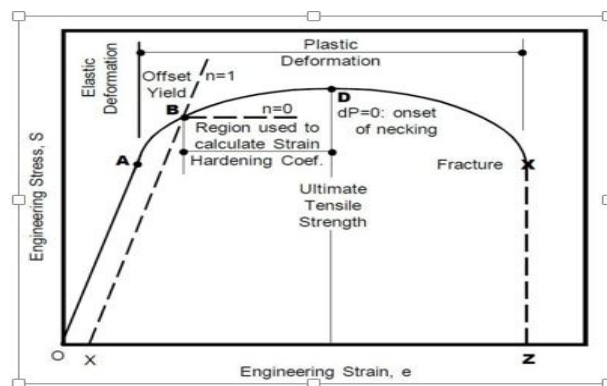


Figure.1: Engineering Stress-

Strain Diagram

II. METHODOLOGY AND SAMPLE PREPARATION

The material is extruded in the form of bar and then solution treated at 530°C.

Aluminium alloy 2618 is an Al-Cu alloy having chemical composition listed below.

Found by XRF

Weight %	Cu	Mg	Si	Fe	Ni	Ti	Zn	Al
AA 2618	2.0	0.8	0.7	1.4	1.3	0.1	-	remaining.

The engineering tensile test also known as tension test is widely used to provide basic design information on the strength of material and as an acceptance test for the specification of the materials. Tensile tests are simple, relatively inexpensive, and fully standardized. By pulling on something, it can be very quickly determined how the material will react to forces being applied in tension. As the material is being pulled, its strength along with how much it will elongate can be found out. A lot about a substance can be learned from tensile testing. As the machine continues to pull on the material until it breaks, a good, complete tensile profile is obtained. A curve will result showing how it reacted to the forces being applied. In the tensile test a specimen is subjected to a continually increasing uniaxial tensile force while simultaneous observations are made of the elongation of the specimen.

1) *High Cycle Fatigue Test:* High-cycle fatigue involves a large number of cycles ($N > 10^5$ cycles) and an elastically applied stress. High-cycle fatigue tests are usually carried out for 10^7 cycles and sometimes 5×10^8 cycles for nonferrous metals. Although the applied stress is low enough to be elastic, plastic deformation can take place at the crack tip. High-cycle fatigue data are usually presented as a plot of stress, S , versus the number of cycles to failure, N . A log scale is used for the number of cycles. The value of stress, S , can be the maximum stress, σ_{max} , the minimum stress, σ_{min} , or the stress amplitude, σ_a . The S-N relationship is usually determined for a specified value of the mean stress, σ_m , or one of the two ratios, R or A . The fatigue life is the number of cycles to failure at a specified stress level, while the fatigue strength (also referred to as the endurance limit) is the stress below which failure does not occur. As the applied stress level is decreased, the number of cycles to failure increases. Normally,

the fatigue strength increases as the static tensile strength increases. It should be noted that there is a considerable amount of scatter in fatigue test results. It is therefore important to test a sufficient number of specimens to obtain statistically meaningful results. Fatigue cracking can occur quite early in the service life of the component by the formation of a small crack, generally at some point on the external surface.

Cyclic stress range: $\Delta\sigma = \sigma_{max} - \sigma_{min}$

Cyclic stress amplitudes: $\sigma_a = \frac{\sigma_{max} - \sigma_{min}}{2}$

Mean stress: $\sigma_m = \frac{\sigma_{max} + \sigma_{min}}{2}$

Stress ratio: $R = \frac{\sigma_{min}}{\sigma_{max}}$

Amplitude ratio: $A = \frac{\sigma_a}{\sigma_m} = \frac{1 - R}{1 + R}$

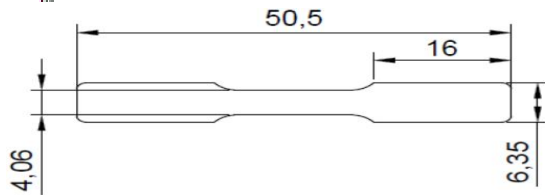


Figure.2: Fatigue specimen ASTM standard(mm)

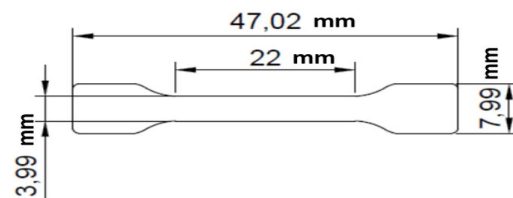


Figure.3: Tensile specimen ASTM standard(mm)

III. RESULTS AND ANALYSIS

The tensile test results at 10^{-3} strain rate for two different heat treatments have been collected at different temperature ranges and stress strain curve has been plotted.

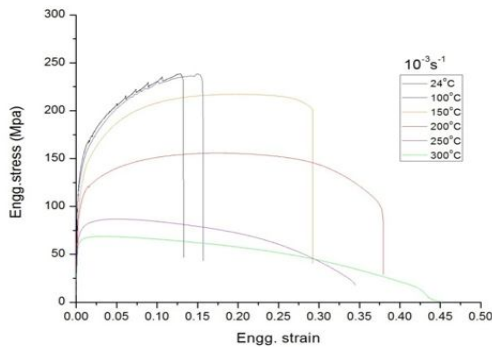


Figure.4: Stress strain diagram at 10^{-3} rate Solution treated condition

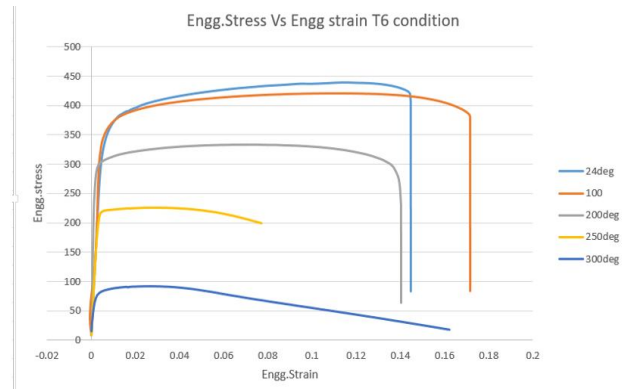


Figure.5: Stress strain diagram at 10^{-3} rate for T6 condition

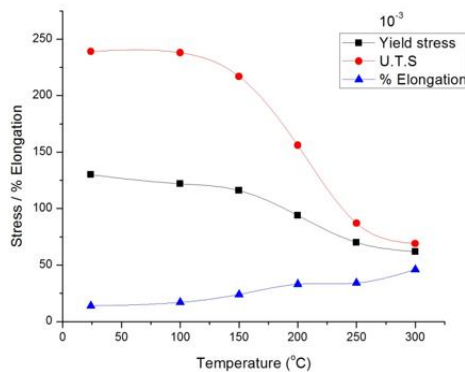


Figure.6: Temperature effect on yield stress, UTS, % elongation at 10^{-3} rate.

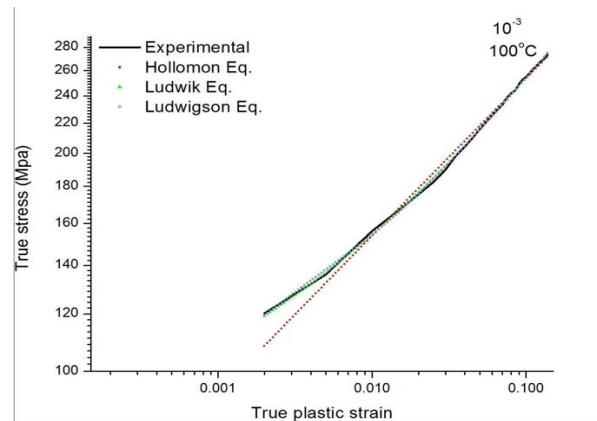


Figure 7: Curve fitting for 100deg 10^{-3} strain rate of AA2618.

The data obtained from engineering stress and strain curve up to the onset of necking were converted into true stress and true strain data according to:

$$\sigma = s(\epsilon + 1)$$

$$\epsilon = ln(\epsilon + 1)$$

The strain hardening exponent (n) for monotonic tensile loading of aero engine metallic ductile material (AA2618) was calculated from elastic modulus, 0.2% proof stress, and ultimate tensile strength.

The constituent relationships are used to approximate the plastic deformation, i.e. Hollomon, Ludwik, Ludwigs relationships and plotted as shown in figure 7.

Fitting Equation	Test temperature (°C)	k ₁ , MPa	n ₁	k ₂	n ₂	Value of χ^2
Hollomon	100	428.46	0.24	0	0	12.34
Ludwik		388.5	0.35	0	0	1.98
Ludwigson		429.8	0.22	3.21	-119	1.01

Table 1: Flow parameter values at 100 deg, 10⁻³ strain rate of AA2618.

Hollomon equation: $\sigma_H = K_H \epsilon^{n_H}$

Ludwik equation: $\sigma = \sigma_0 + K \epsilon^n$

Ludwigson Equation: $\sigma_H = K_H \epsilon^{n_H} + e^{(K_L + n_L \epsilon)}$

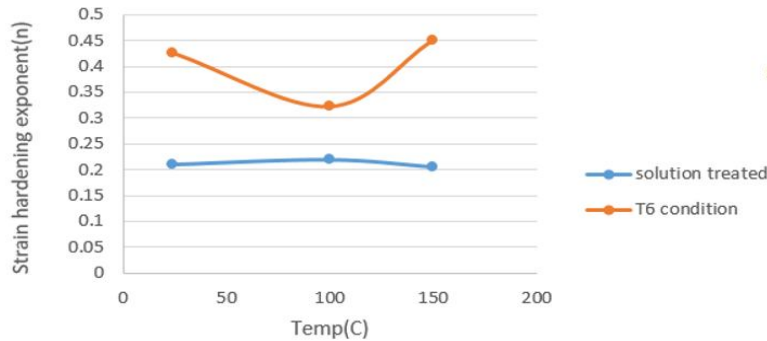


Figure 8: Strain hardening exponent comparison.

The strain hardening exponent (n) determines how the metal behaves when it is being formed. Materials that have higher n values have better formability than those with low n values. As metals work harden, their remaining capacity for work hardening decreases. This means that high strength tempers of a given material typically would have lower n values than lower strength tempers of the same alloy. However, since these coefficients are derived from curve fitting, these trends will not necessarily hold true in reality. It is the measure of increase in hardness and strength caused by plastic deformation.

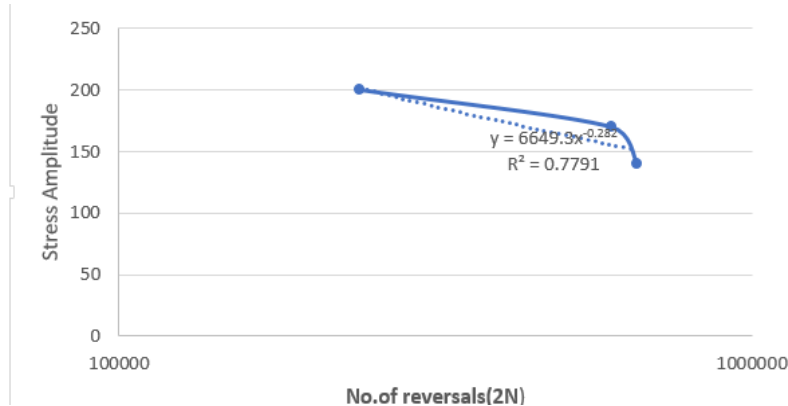


Figure 9: High cycle fatigue results.

IV. CONCLUSION

The results of solution treatment indicate that the mechanical properties of Al-Cu alloy increase and then decrease with the increase of solution temperature. This is because the residual phases dissolve gradually into the matrix, and the fraction of the precipitation and the size of the re-crystallized grain increased. Compared to the solution temperature, the solution holding time has less effect on the microstructure and the mechanical properties of Al-Cu alloy.

The artificial aging treatments were conducted at 160–180 °C for 2–8 h. The results show that the ultimate tensile strength can be obtained at 180 °C for 8 h. Ultimate tensile strength increased with increasing time or temperature. Yield strength was found as the same as the ultimate tensile strength result.

Also comparison of strain hardening exponent for artificially aged and naturally aged indicates that artificially aged will have more formability than naturally aged. This is due to the dispersion of precipitates inside the Al matrix which promote the movement of dislocations

REFERENCES

- [1] R. N. Wilson, P. J. E. Forsyth, Effects of Additions of 1% Iron and 1% Nickel on Age Hardening of an Aluminum-2.5% Copper-1.2% Magnesium Alloy. *Journal of the institute of metals* 94, 8 (1966).
- [2] W. Feng, X. Baiqing, Z. Yongan, L. Zhihui, L. Peiyue, Microstructural characterization of an Al-Cu-Mg alloy containing Fe and Ni. *Journal of Alloys and Compounds* 487, 445 (2009).
- [3] G. Wang, B. Xiong, Y. Zhang, Z. Li, P. Li, Microstructural characterization of as-cast and Homogenized 2D70 aluminium alloy. *International Journal of Minerals, Metallurgy and Materials* 16,427 (2009).
- [4] I. N. A. Oguocha, S. Yannacopoulos, Y. Jin, The structure of Al_xFeNi phase in Al-Cu-Mg-Fe-Ni alloy (AA2618). *Journal of Materials Science* 31, 5615 (1996).
- [5] J.H. Hollomon: *Trans. AIME*, 1945, vol. 162, pp. 268–90.
- [6] P. Ludwik: *Elemente der Technologischen Mechanik*, Springer, Berlin, Germany, 1909, pp. 32–37.
- [7] D.C. Ludwigson: *Metall. Trans.*, 1971, vol. 2 (10), pp. 2825–28.



10.22214/IJRASET



45.98



IMPACT FACTOR:
7.129



IMPACT FACTOR:
7.429



INTERNATIONAL JOURNAL FOR RESEARCH

IN APPLIED SCIENCE & ENGINEERING TECHNOLOGY

Call : 08813907089  (24*7 Support on Whatsapp)